Society For Biomaterials

The use of SHP-2 gene transduced bone marrow mesenchymal stem cells to promote osteogenic differentiation and bone defect repair in rat

Dapeng Fan,[1†] Shen Liu,[1†] Shichao Jiang,[2†] Zhiwei Li,[1] Xiumei Mo,[3] Hongjiang Ruan,[1] Gang-Ming Zou,[4] Cunyi Fan[1]

[1]Department of Orthopaedics, Shanghai Jiaotong University Affiliated Sixth People's Hospital, 600 Yishan Road, Shanghai 200233, People's Republic of China
[2]Department of Orthopaedics, Shandong Provincial Hospital Affiliated to Shandong University, No.324 Jingwu Road, Jinan, 250021, Shandong, People's Republic of China
[3]College of Chemistry, Chemical Engineering and Biotechnology, Donghua University, Shanghai 201620, China
[4]Hawaii Gangze Inc, 421 Nahua Street, Suite 146, Honolulu, Hawaii 96815

Received 8 January 2016; revised 23 February 2016; accepted 10 March 2016
Published online 30 March 2016 in Wiley Online Library (wileyonlinelibrary.com). DOI: 10.1002/jbm.a.35718

Abstract: Bone tissue engineering is a promising approach for bone regeneration, in which growth factors play an important role. The tyrosine phosphatase Src-homology region 2-containing protein tyrosine phosphatase 2 (SHP2), encoded by the PTPN11 gene, is essential for the differentiation, proliferation and metabolism of osteoblasts. However, SHP-2 has never been systematically studied for its effect in osteogenesis. We predicted that overexpression of SHP-2 could promote bone marrow-derived mesenchymal stem cell (BMSC)osteogenic differentiation and SHP-2 transduced BMSCs could enhance new bone formation, determined using the following study groups: (1) BMSCs transduced with SHP-2 and induced with osteoblast-inducing liquid (BMSCs/SHP-2/OL); (2) BMSCs transduced with SHP-2 (BMSCs/-SHP-2); (3) BMSCs induced with osteoblast-inducing liquid (BMSCs/OL) and (4) pure BMSCs. Cells were assessed for osteogenic differentiation by quantitative real-time polymerase chain reaction analysis, western blot analysis, alkaline phosphatase activity and alizarin red S staining. For *in vivo* assessment, cells were combined with beta-tricalcium phosphate scaffolds and transplanted into rat calvarial defects for 8 weeks. Following euthanasia, skull samples were explanted for osteogenic evaluation, including micro-computed tomography measurement, histology and immunohistochemistry staining. SHP-2 and upregulation of its gene promoted BMSC osteogenic differentiation and therefore represents a potential new therapeutic approach to bone repair. © 2016 Wiley Periodicals, Inc. J Biomed Mater Res Part A: 104A: 1871–1881, 2016.

Key Words: SHP-2, Osteogenesis, Bone repair, Tissue engineering, BMSCs, β-TCP

How to cite this article: Fan D, Liu S, Jiang S, Li Z, Mo X, Ruan H, Zou G-M, Fan C. 2016. The use of SHP-2 gene transduced bone marrow mesenchymal stem cells to promote osteogenic differentiation and bone defect repair in rat. J Biomed Mater Res Part A 2016:104A:1871–1881.

INTRODUCTION

Bone tissue exhibits a powerful regeneration capacity in fracture patients. However, bone repair is severely limited when large bone defects occur in cases of severe trauma, surgical intervention, sizable infection and cancer morbidity, to name a few. Autogenous bone graft is considered the gold standard for the repair of bone defects. With developments in microsurgery, application of the pedicled bone flap has improved the survival rate of bone grafts.[1,2] Nevertheless, disadvantages of this approach include infection, pain, loss of function, and restricted supply owing to donor shortage.[3]

Bone tissue engineering represents a promising approach to bone repair and has undergone substantial development over the last few decades.[4] Growth factors are critical for the proliferation and osteogenic differentiation of the chosen cell source, therefore research has been focused on identifying candidate gene targets.[5,6] To date, various cytokines and growth factors, including bone morphogenetic protein-2 (BMP-2),[7] basic fibroblast growth factor (bFGF),[8] and hypoxia-inducible factor-1α (HIF-1α),[9] have been proven to be efficient in promoting osteogenesis. However, application of BMP-2 has reported complications, including early inflammatory reaction and osteolysis, ectopic bone

Dapeng Fan, Shen Liu, and Shichao Jiang contributed equally to this work.
Correspondence to: C.Fan; Department of Orthopaedics, Shanghai Jiaotong University Affiliated Sixth People's Hospital, 600 Yishan Road, Shanghai 200233, PR China. e-mail: fancunyi888@hotmail.com; H. Ruan; Department of Orthopaedics, Shanghai Jiaotong University Affiliated Sixth People's Hospital, 600 Yishan Road, Shanghai 200233, PR China. e-mail: ruanhongjiang@126.com; G.-M. Zou; Hawaii Gangze Inc. 421 Nahua Street, Suite 146, Honolulu, HI 96815. e-mail: gz2003@yahoo.com
Contract grant sponsor: Nano-tech Foundation of Shanghail; contract grant number: 1052nm0570045 and 11nm0503100
Contract grant sponsor: National Natural Science Foundation of China; contract grant number: 51003058

formation—in some cases leading to compression of neural elements, seroma formation, and a possible increased risk of malignancy.[10,11] Unregulated bFGF signaling is closely related to tumor angiogenesis,[12] while HIF-1α is reported to be a major driver of acute inflammation.[13] In addition, there remains a growing socio-economic need for more effective strategies to repair damaged bone.[14]

Src homology region 2 (SH2)-containing protein tyrosine phosphatase 2 (SHP-2), encoded by the PTPN11 gene, is a nonreceptor phosphotyrosine phosphatase.[15] SHP-2 is widely expressed in human tissues, especially in the heart, brain, skeletal and muscular systems. The SHP-2 gene play a critical role for embryonic stem cell differentiation into all blood cell lineages, cardiac muscle cells, and neuronal/glial cells.[16] Recently, SHP-2 has been proven to be essential for osteoblast differentiation, proliferation and metabolism.[17,18] Individual SHP-2 missense mutations are highly specific to Noonan syndrome (NS), an autosomal dominant disorder characterized mainly by skeletal dysplasia.[19,20] Furthermore, SHP-2 knockout mice exhibit postnatal bone growth retardation, limb and chest deformity, and calvarial defects.[21] Despite this, the potential effect of SHP-2 in promoting bone marrow-derived mesenchymal stem cell (BMSC) osteogenic differentiation remains to be elucidated. Moreover, no published data exists on the use of SHP-2 gene transduced stem cells for bone repair, until now.

In our previous research, we showed the importance of SHP-2 function for controlling normal hematopoiesis.[22] The excellent degradability and bioactivity properties of β-tricalcium phosphate (β-TCP) have also been shown in our previous research.[23] BMSCs are frequently used as a cell source for bone tissue engineering because of their multipotency, relative abundance and rapid expansion.[24–26] In this study therefore, BMSCs and β-TCP scaffolds were used as the cell source and carrier, respectively. Based on our previous research, we aimed to evaluate the feasibility and efficacy of SHP-2 on BMSCs osteogenic differentiation and SHP-2 transduced BMSCs on the promotion of bone repair. No additional exogenous growth factors were added to enable a clear understanding of the effect of SHP-2 overexpression on bone repair.

MATERIALS AND METHODS

Materials

Beta-TCP (β-TCP) was purchased from Bio-Lu (China). Dulbecco's modified Eagle's medium (DMEM) and fetal bovine serum (FBS) were both purchased from Gibco (Grand Island, NY, USA). All other reagents and media were reagent grade or better and were purchased from Invitrogen (California, USA), unless otherwise indicated.

Isolation and culture of rat BMSCs

Sprague Dawley (SD) rats were provided by the Shanghai Animal Experimental Center, and all procedures were approved by the Animal Research Committee of the Sixth People's Hospital, Shanghai Jiao Tong University School of Medicine. Total BMSCs were isolated from the femoral marrow cavity of 7-day-old male SD rats as described previously by Liu et al.[27] Briefly, primary cells were cultured in DMEM containing 10% FBS and 100 U/mL penicillin for 5 days. The medium was then changed and was renewed every 3 days. On reaching 90% confluence, BMSCs were released from the culture substratum using trypsin/EDTA (0.25% w/v trypsin, 0.02% EDTA) and re-seeded into dishes (10 cm in diameter) at 1.0×10^5 cells/mL in 10 mL/dish at cultured 37°C in 5% CO_2 atmosphere.

Lentiviral vector construction and transduction

RNA extracted from SD rat liver cells was used to generate cDNA by reverse transcription polymerase chain reaction (PCR) using a PrimeScript RT Reagent Kit (TaKaRa, Dalian, China) as previously described.[6] The SHP-2 gene was amplified by PCR using the following primers: 5′-CCC (Protective base) AAGCTT (*Hin*dIII) GCCACC (Kozak) ATGACATCCCGGAGATGGTTTCA-3′ (Forward) and 5′-CG (Protective base) GGATCC (BamHI) CATCTGAAACTCCTCTGCTGC-3′ (Reverse), which were designed by Oligo 6.0 software. The amplification parameters were as follows: 32 cycles of denaturation at 95°C for 10 s, annealing at 58°C for 30 s and extension at 72°C for 120 s. SHP-2 was subcloned into the pCDH-CMV-MCS-EF1-copGFP expression lentivector (System Biosciences) and sequencing was used to confirm the vectors constructed.

293TN producer cells were co-transfected with pPACK Packaging Plasmid Mix (System Biosciences) and expression lentivector (containing SHP-2) or control green fluorescent protein (GFP) plasmid using Lipofectamine™ 2000 (Invitrogen).[28] Forty-eight hours later, the supernatant was harvested and then cleared by centrifugation at 5000×*g* at 4°C for 5 min, and passed through a 0.45 μm PVDF membrane(-Millipore, MI). The titer of virus was determined by gradient dilution. The packaged lentiviruses were named as Lv- SHP-2 and Lv-GFP. For transduction, cells were incubated with the virus and 8 mg/ml polybrene for 24 h. Lentiviruses were added to reach a multiplicity of infection (MOI) of 50 for 72 h. The transfection efficiency of the lentiviral vectors was reflected by the GFP-positive proportion of BMSCs detected using flow cytometry. Cells induced with osteoblast-inducing liquid (OL) acted as controls. OL consists of DMEM supplemented with 5% FBS and 200 ng/mL rhBMP-2 (R&D Systems, Minneapolis, MN) and the liquid was changed every 2–3 days. This study was designed to include four groups: (1) BMSCs transfected with SHP-2 and induced with osteoblast-inducing liquid (OL) (BMSCs/SHP-2/OL group); (2) BMSCs infected with SHP-2 only (BMSCs/-SHP-2 group); (3) BMSCs induced with OL only (BMSCs/OL group); and (4) pure BMSCs (BMSC group).

Quantitative real-time PCR (qPCR) analysis

Total cellular RNA was extracted from BMSCs on days 0, 1, 4, 7, 10, 14, and 21 after gene transduction with an RNeasy Mini kit (Qiagen, Germany). The quality and quantity of the extracted RNA were examined by spectrophotometric analysis using a biophotometer (Eppendorf Biophotometer Plus). Reverse transcription was carried out on 1 μg of total RNA in a final volume of 20 μL using a PrimeScript RT reagent

TABLE I. Nucleotide Sequences for Real-Time RT-PCR Primers

Genes	Primer sequence(5′–3′) (forward/reverse)	Annealing temperature (°C)	Product size (bp)	Accession number
Beta actin	GCATGGGCCAGAAGGACTCGTA TCGCGGTTGGCCTTGGGGTTCA	60	214	NM_001101683.1
Ikaline phosphatase (ALP)	CGGTGGTGCTGGCGGTGGAC GCGGCCTCGTGCGTGCTCTC	60	209	XM_002709498.1
Osteocalcin	AGGGCCCTCACTCTTGTCGCGCCG GGCTCGCTTCAC	60	149	XM_002715383.
Runx 2	CCCCGGGAACCCAGAAGGCACAG ACATAGGACCACGGCGGGGAAGACT	60	229	XM_002714704.1

kit (Takara Bio, Shiga, Japan) according to the manufacturer's recommendations. The relative expression of each target mRNA was obtained by the comparative ΔC_t method as previously described.[29] Gene-specific primers were synthesized commercially (Shengong, Shanghai, China). All genes, primer sequences, annealing temperatures, product sizes, and accession numbers are listed in Table I. All experiments were performed in triplicate. All values were normalized to glyceraldehyde 3-phosphate dehydrogenase (GAPDH), and all data are shown as the average ± standard deviation (SD).

Western blot analysis

Cells (1.0×10^5/well) were seeded into six-well plates 1 day before transduction. Protein was collected from cultured cells on days 0, 1, 4, 7, 10, 14, and 21 after gene transduction. Protein concentrations were measured using the DC Protein Assay kit (Invitrogen) after cell lysis. Equal amounts of protein (15 μg per lane) were separated on duplicate 8–10% SDS–PAGE gels and transferred to a polyvinylidene difluoride (PVDF) membrane (0.45 μm, Millipore, Bedford, MA). Membranes were incubated with specific primary antibodies (1:600 dilution) overnight at 4°C. Membranes were then washed three times with tris-buffered saline (TBS) containing 0.1% tween-20 detergent and incubated for 2 h with horseradish peroxidase (HRP)-conjugated secondary antibodies. The Enhanced Chemiluminescence System (ECL, Amersham Pharmacia Biotech, USA) and Kodak X-OMAT Film (Rochester, New York, USA) were used to visualize protein bands. The same procedure was used for antibodies against other proteins, including β-actin, alkaline phosphatase (ALP), osteocalcin (OCN), and runt-related transcription factor 2 (Runx2). Relative protein levels were normalized against β-actin. All experiments were performed in triplicate. Data are shown as the mean ± SD.

Alkaline phosphatase (ALP) activity and alizarin red S (ARS) staining

Cells from each of the aforementioned groups (1×10^6 cells) per well were plated into six-well culture plates. Cells were then cultured for 3 days and ALP staining was performed using the alkaline phosphatase detection kit (Chemicon, Temecula, CA) according to the manufacturer's instructions.[30] ALP activity was then calculated with the Lab Assay ALP kit (Bioassay Systems, CA, USA) according to the manufacturer's instructions. A Bio-Rad Assay Kit (BioRad Laboratories, Hercules, CA) was then used to measure the protein concentration of the lysates, and then ALP activity was quantified by protein concentration.

For ARS staining, cells from each of the four groups were plated in triplicate in six-well culture plates, cultured for 14 days and fixed in 70% ethanol. ARS staining was performed in accordance to a previous report.[31] Newly formed calcium nodules with a diameter >1 mm were counted and analyzed.

BMSCs seeding in β-TCP scaffolds

Disc-shaped (Φ6 mm × 2 mm^3) porous β-TCP scaffolds with an average pore size of 500 μm and 75% porosity were used. BMSCs/SHP-2OL, BMSCs/SHP-2, BMSCs/OL, and BMSC group cells were seeded on to the scaffolds in accordance with the methods described previously.[9] In brief, BMSCs were detached from the culture dishes, centrifuged to remove the supernatant and then resuspended in serum-free DMEM at a density of 2.0×10^5 cells/mL. The cells were then seeded at a density of 1.0×10^5 cells/mL on to each β-TCP under sterile conditions and incubated for at least 4 h to ensure total absorption. Scaffolds were seeded 24 h prior to implantation into rat cranial defects as described below.

Animal experiments

All animal experimental procedures were approved by the Animal Research Committee of the Sixth People's Hospital, Shanghai Jiao Tong University School of Medicine. All surgical procedures were performed on 12-week-old male SD rats. A 1.0 × 1.5 cm sagittal incision and blunt dissection was made on the scalp and the skull was exposed. Using a 6-mm diameter electric trephine (Nouvag AG, Goldach, Switzerland), two axial-symmetrical circular bone defects were drilled on the symmetrical parietal bone. The cell-seeded scaffolds were then implanted into the defects. Twenty-four rats were randomly divided into the following four research groups ($n = 6$/group): (1) β-TCP with BMSCs/SHP-2/OL; (2) β-TCP with BMSCs/SHP-2; (3) β-TCP with BMSCs/OL; (4) β-TCP/BMSCs. All rats were bred normally after experimental set-up.

Microcomputed tomography (micro-CT)

Postoperatively, animals were euthanized under general anesthesia at 8 weeks, and their skulls were then explanted

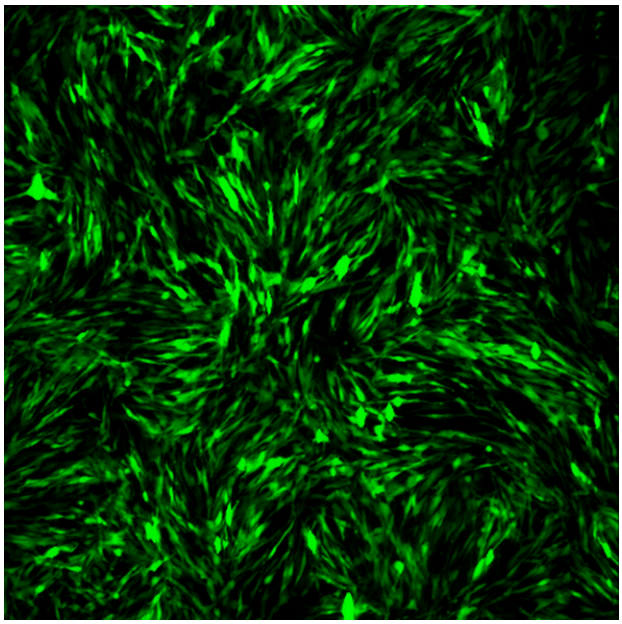

FIGURE 1. Fluorescence images of transfected cells.

and fixed in 4% paraformaldehyde. The subsequent steps taken were in accordance with those described previously.[32] The three-dimensional (3D) superior aspect images and transverse views were generated using Avizo software. Micro-CT images were analyzed using PMOD 3.4 software (Pmod Technologies, Zurich, Switzerland) to calculate indexes including tissue volume (TV), bone volume (BV), directly measured bone volume fraction (BV/TV), trabecular thickness (Tb.Th), and trabecular number (Tb.N).

Histology and immunohistochemistry analysis

The histological method was adapted from one described previously.[7] Briefly, the samples were fixed with 4% neutral buffered formalin (NBF). After dehydration, harvested samples were embedded in paraffin wax. Sagittal sections in the middle of the tissue, representing the central area of each defect was cut with a microtome(Leica, Hamburg, Germany) and were subsequently stained with hematoxylin and eosin (H&E) and Masson's trichrome stain to distinguish cells from surrounding tissues. Immunohistochemical staining was performed with anti-rat osteocalcin (OCN) and osteopontin (OPN) antibodies. Sample sagittal sections were also used for immunohistochemistry which was performed as previously described.[33] Briefly, sections were incubated with 5% bovine serum albumin (BSA) to block nonspecific binding before adding the primary antibodies for 1 h. Secondary antibody (Boster, China) was then added to the sections for 30 min at room temperature prior to incubation with the streptavidin biotin complex (Boster, China) for 20 min. Staining was performed using DAB substrate (Boster, China) and the slides were counterstained with hematoxylin and mounted. A light microscope (Carl Zeiss, Germany) was used to visualize the sections.

Statistical analysis

All experiments were performed in triplicate unless otherwise specified. Experimental data are expressed as means $\pm$ SD and were compared by one-way analysis of variance (ANOVA). Differences at a level of $p < 0.05$ were considered statistically significant.

RESULTS

Gene transduction and SHP-2 expression

Preliminary experiments were performed using various doses of lentivirus to identify the optimal MOI. An MOI of 25 was found to enable an optimal transduction efficiency. Quantification of lentiviral gene transfer efficiency in BMSCs was determined by the fraction of fluorescent cells using fluorescent microscopy. An average of the fraction of green fluorescent cells in five random fields of view was used to estimate the overall fraction of fluorescing cells. A transfer efficiency up to 90% was achieved in all the transfected groups at 48 h after transfection (Fig. 1).

SHP-2 and osteogenic-related protein expression

Overexpression of the SHP-2 gene was evaluated and analyzed by western blot. At each time point, the relative expression level of SHP-2 was significantly upregulated by at least twofold in the BMSCs/SHP-2/OL group compared with all other groups. In addition, the relative expression level of SHP-2 in the BMSCs/SHP-2 group was higher than in the BMSC and BMSCs/OL groups (Fig. 2).

Protein expression of osteogenic-related genes was analyzed by qPCR (Fig. 3) and western blot (Fig. 4) to indicate the differences between groups and culture time points. Both qPCR and western blot were carried out on days 0, 1, 4, 7, 10, 14, and 21 of culture and the results supported each other. The BMSCs/SHP-2/OL group demonstrated a notably higher level of expression for all three osteogenic markers compared with the other three groups at each time point. The BMSCs/SHP-2 group showed the second highest level of expression, although with respect to expression of OCN, the BMSCs/OL group was comparable to the BMSCs/SHP-2 group [Fig. 3(B)]. Expression of OCN was similar in BMSCs/SHP-2 and BMSCs/SHP-2/OL groups [Fig. 4(C)]. The BMSCs group had the lowest osteogenic marker expression levels at all time points compared with the other three groups (Figs. 3 and 4). These results indicate that important osteogenic factors (ALP, OCN, Runx2) were significantly unregulated by overexpression of SHP-2 in BMSCs.

ALP and ARS

Cells from each groups were evaluated for ALP activity on days 7 and 14 and ARS on days 14 and 21. A significant increase in ALP expression was seen in the BMSCs/SHP-2/OL group from day 7 to 14, with very little change observed for the BMSC group for both ALP and ARS staining. ALP and ARS staining was enhanced in the BMSCs/SHP-2 group compared with the BMSCs/OL group [Fig. 5(A)]. Quantification analysis showed that ALP activity and calcium nodule formation in the BMSCs/SHP-2/OL group was at least 3.4-fold greater than in the BMSCs group [Fig. 4(B,C)]. Taken

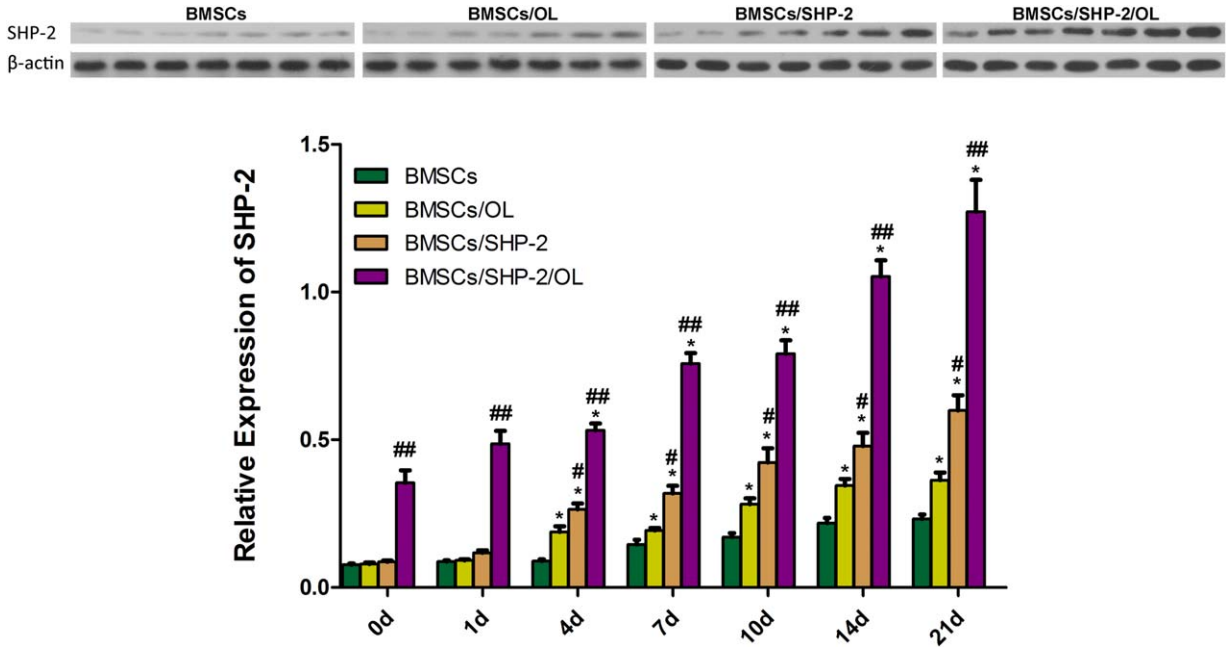

FIGURE 2. The revelative expression of SHP-2 was detected with western blot. Group BMSCs/SHP-2/OL demonstrated an apparent higher level of SHP-2 compared with the other three groups ($^{\#\#}p < 0.05$, Group BMSCs/SHP-2/OL compared with the other three groups; $^{**}p < 0.05$, Group BMSCs/SHP-2 compared with Group BMSCs and BMSCs /OL; $^{*}p < 0.05$, Group BMSCs /OL compared with Group BMSCs).

together, these findings indicate that SHP-2 positively regulates osteogenic differentiation in BMSCs.

Micro-CT measurement

Rat calvarial bone repair was evaluated by micro-CT analysis. For this analysis, four samples were selected randomly from each of the four groups. Photography images show a high-density shadow in most of the β-TCP pores, especially in the transverse aspect. Radiotransparent areas were greatest in the BMSC group compared with all other groups. Differences between the BMSCs/SHP-2 and BMSCs/OL groups were not distinguishable by the naked eye [Fig. 6(A)]. From the quantification view, however, BMD [Fig. 6(B)] and BV/TV [Fig. 6(C)] were higher in the BMSCs/SHP-2 group. With respect to TB.Th [Fig. 6(D)] and TB.N [Fig. 6(E)], however, the two groups were comparable. In summary, these data indicate that SHP-2 transduced BMSCs effectively promoted new bone formation and the radiographic results indicate that SHP-2 transduced BMSCs promoted new bone formation in β-TCP scaffolds.

Histology and immunohistochemistry

H&E [Fig. 6(A)] and Masson trichrome [Fig. 7(B)] staining of tissue slices confirmed that although new bone formation was observed in all experimental groups, greater bone infill was observed in the BMSCs/SHP-2/OL group. For the BMSCs/SHP-2/OL group, β-TCP pores were bridged with newly formed bone and fibrous connective tissues [Fig. 7(A4) and (A^8)]. Considerably more newly formed bone tissue was also observed in the BMSCs/SHP-2 group [Fig. 7(A3) and (A^7)]. Newly formed bone was much sparser in the BMSCs/OL group [Fig. 7(A2) and (A^6)]. Finally,

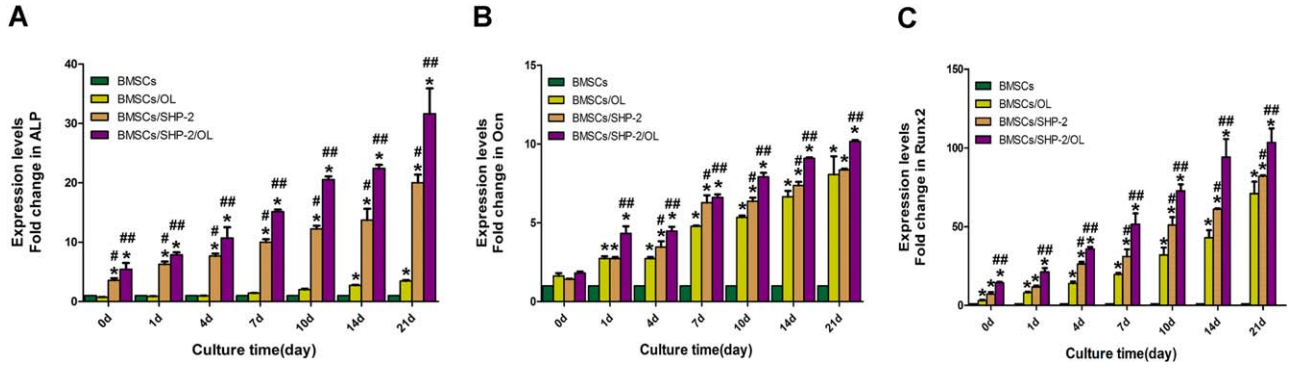

FIGURE 3. Expression of osteogenic markers' fold changes in the four groups by quantitative real-time PCR. A: ALP, B: OCN, C: Runx2 ($^{\#\#}p < 0.05$, Group BMSCs/SHP-2/OL compared with the other three groups; $^{**}p < 0.05$, Group BMSCs/SHP-2 compared with Group BMSCs and BMSCs /OL; $^{*}p < 0.05$, Group BMSCs/OL compared with Group BMSCs).

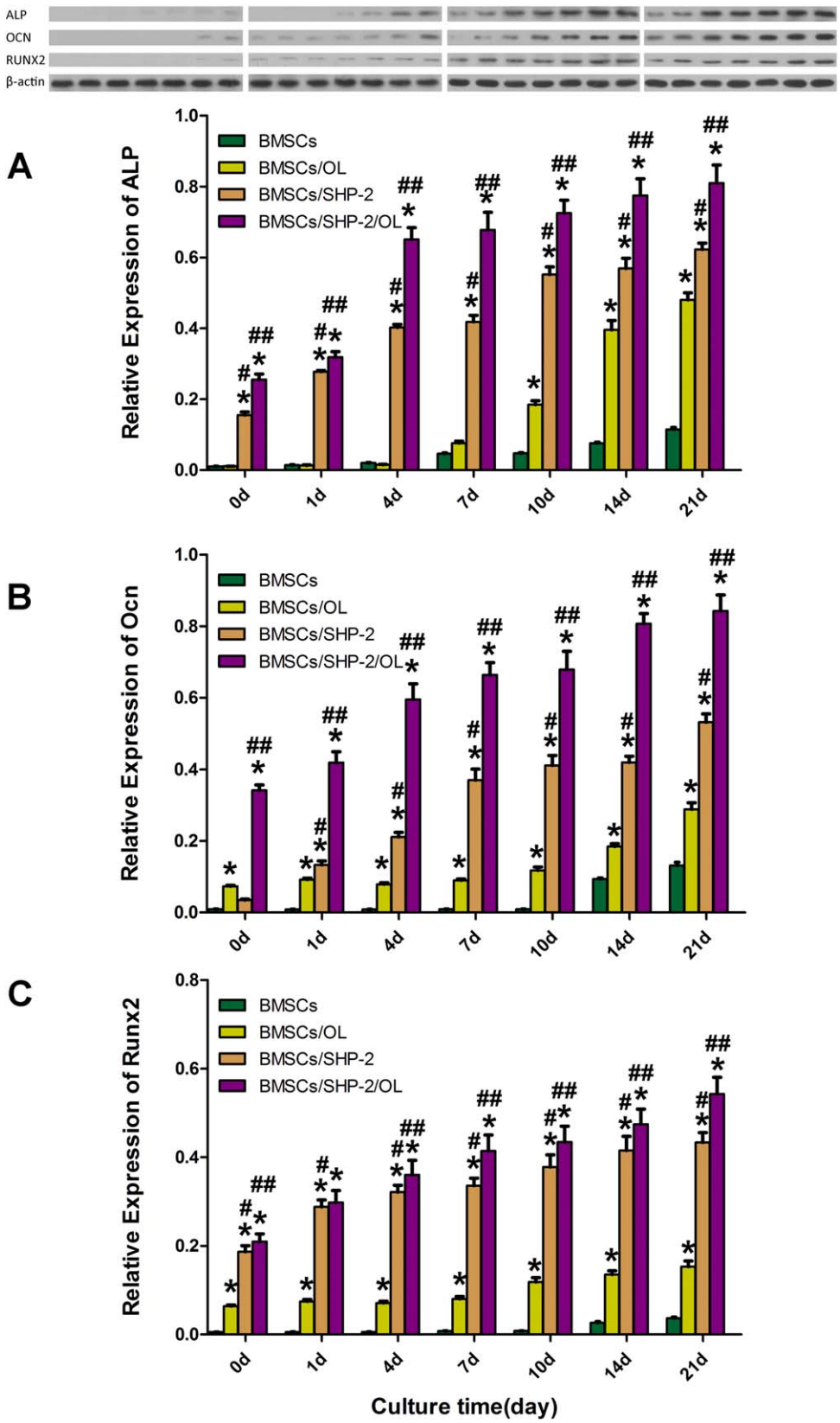

FIGURE 4. Relative expression of osteogenic markers by western blot analysis (A), ALP (B), OCN (C), Runx2 ($^{\#\#}p < 0.05$, Group BMSCs/SHP-2/OL compared with the other three groups; $^{**}p < 0.05$, Group BMSCs/SHP-2 compared with Group BMSCs and BMSCs/OL; $^{*}p < 0.05$, Group BMSCs/OL compared with Group BMSCs).

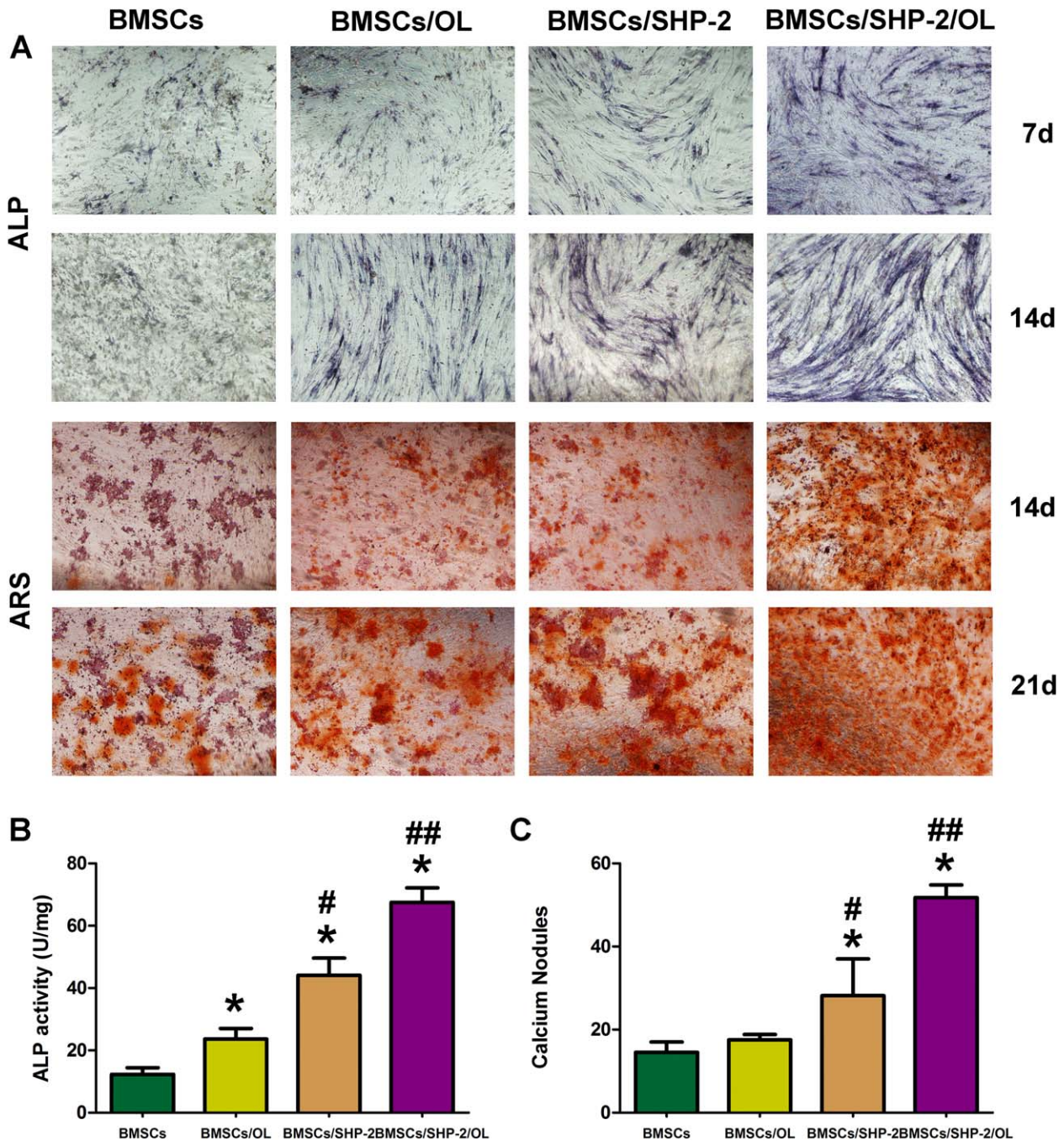

FIGURE 5. Detection of osteogenic sign by ARS staining on days 14 and 21 and ALP staining on days 7 and 14. A: ALP and ARS activity, B: quantification of ALP activity, C: quantification of calcium nodules ($^{\#\#}p < 0.05$,GroupBMSCs/SHP-2/OL compared with the other three groups; $^{**}p < 0.05$, Group BMSCs/SHP-2 compared with Group BMSCs and BMSCs /OL; $^{*}p < 0.05$, Group BMSCs /OL compared with Group BMSCs).

regeneration of new bone was very rare in the BMSC group [Fig. 7(A1) and (A^5)].

Immunohistochemical staining [Fig. 7(C)] revealed a similar result to H&E and Masson staining with positive expression of OCN and OPN being largely observed in the BMSCs/SHP-2/OL group [Fig. 7(C4) and (C^8)]. Conversely, expression levels of OCN and OPN were negligible in the BMSC group [Fig. 7(C1) and (C^5)]. In summary, these results more vividly show that SHP-2 transduced BMSCs could effectively promote osteogenesis.

DISCUSSION

To date, research into SHP-2 has been increasingly focused on its regulation of bone and skeletal development.[17,21,34] In view of sporadic research studies on the relevance of the SHP-2 gene for osteoblast differentiation and significant reports regarding the association between dysosteogenesis and SHP-2 gene mutation, we hypothesized that overexpression of SHP-2 could promote BMSCs osteogenic differentiation and that SHP-2 transduced BMSCs could promote bone

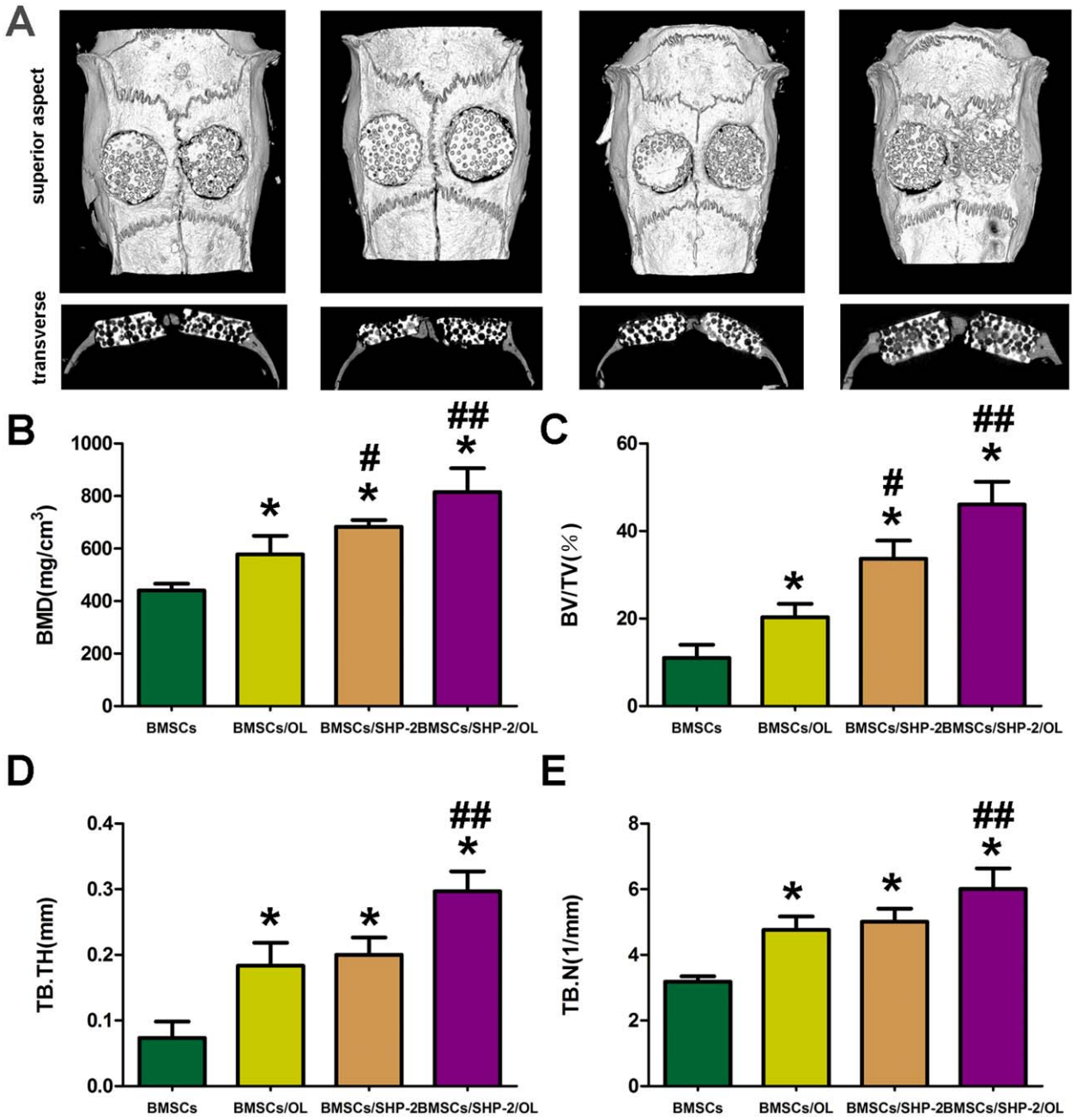

FIGURE 6. Micro-CT evaluation of calvarial bone healing. Quantitative analysis of new bone formation area for bone mineral density (BMD), directly measured bone volume fraction (BV/TV), trabecular thickness (Tb.Th), and trabecular number (Tb.N) ($^{\#\#}p < 0.05$, GroupBMSCs/SHP-2/OL compared with the other three groups; $^{**}p < 0.05$, Group BMSCs/SHP-2 compared with Group BMSCs and BMSCs/OL; $^{*}p < 0.05$, Group BMSCs/OL compared with Group BMSCs).

repair. To prove the validity of SHP-2 in promoting osteogenic differentiation and promoted bone formation, cells induced with OL was set as controls. The main component of OL is BMP-2. In 1965, Urist et al. introduced for the first time that BMPs can lead to bone formation when implanted in an ectopic site.[35] The ectopic bone was the result of osteogenic differentiation of circulating osteoblast progenitors or stem cells, which were locally exposed to the BMP-2. Subsequent studies have also shown that BMP-2 could induces bone regeneration which makes BMP-2 one of the most prevalent growth factors in clinical use for bone regeneration.[36–38] Yet, BMP-2 delivered in super-physiological doses may also lead to unfavorable side effects, including excessive bone formation and adverse immune responses.[39,40] As clinical drawbacks of using BMP-2, there are concomitant efforts to search alternative growth factor.

We evaluated the effect of SHP-2 to promote osteogenic differentiation *in vitro*, and SHP-2 transduced BMSCs for tissue-engineered bone repair. Our experimental results supported our initial hypothesis. Our findings demonstrate that

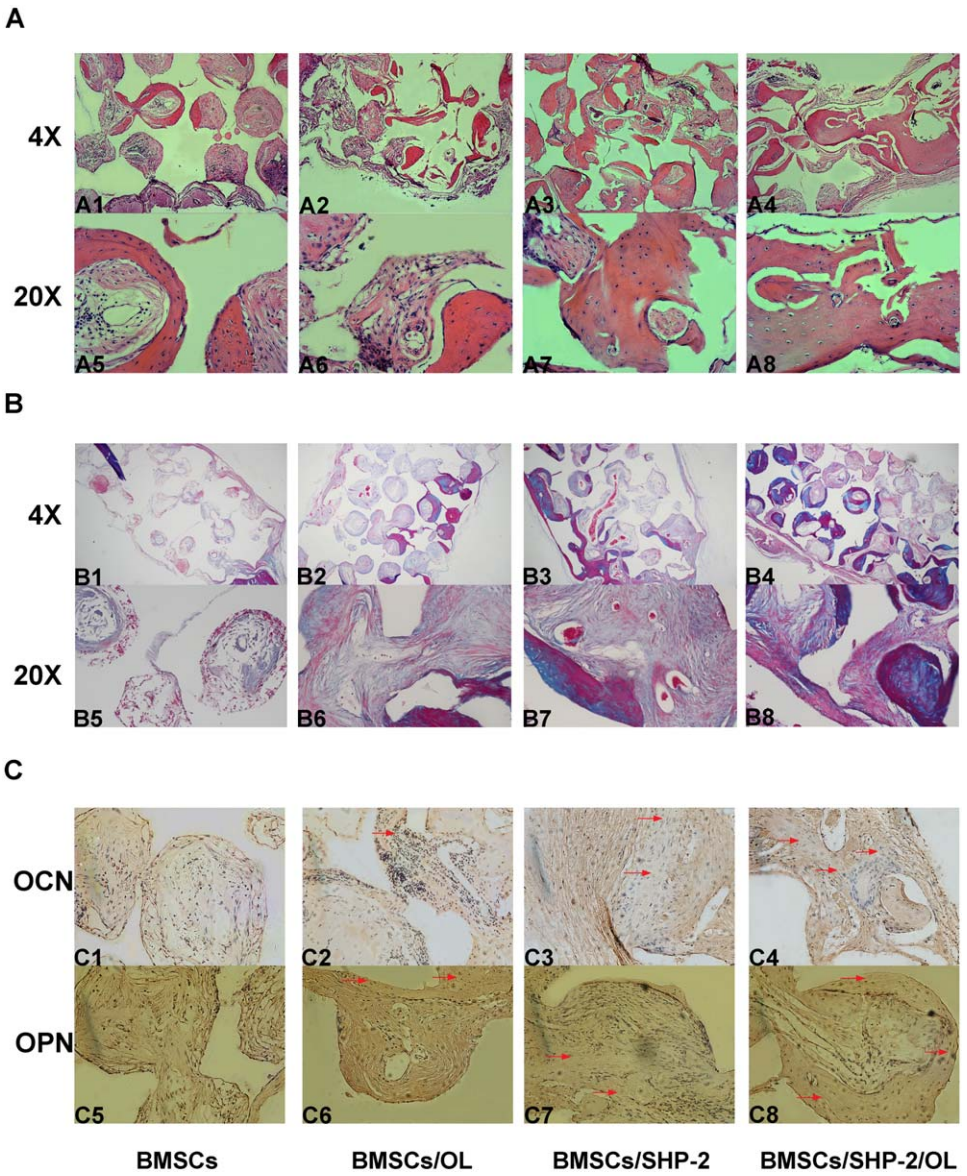

FIGURE 7. Histology and immunohistochemistry. A: H&E staining for tissue sections and original magnification (40× and 200×). B: Masson staining for tissue sections and original magnification (40× and 200×). C: Immunohistochemical staining specific for osteocalcin (OCN) and osteopontin (OPN). Red arrows indicate positive brown staining in new formed bone matrix.

both *in vitro* and *in vivo*, BMSCs/SHP-2 group presented a more favorable osteogenic differentiation and promoted bone formation compared with the BMSCs/OL group. Previous experiments have confirmed that BMSC induced by OL could promotes osteogenesis. In this study, we found that there was a synergistic effect between OL and SHP-2 gene, which further enhanced osteogenesis and bone regeneration, and provided a promising choice for bone tissue engineering.

We postulate that the promotion of osteogenesis by SHP-2 is attributed to the following two reasons. Firstly, SHP-2 could promote signal transduction in the ERK related pathway for osteogenic differentiation. Previous reports demonstrate a role for the ERK pathway in osteogenic differentiation.[41,42] Furthermore, Chen et al. found that defective terminal differentiation caused by the reduced activity of ERK may account for the development of enchondromas in PTPN11-mutant mice, and concluded that the ERK/MAPK signaling pathway, which can be promoted by SHP-2, plays a crucial role in bone terminal differentiation.[43] That is to say, SHP-2 could promote osteogenic differentiation by promoting the signal transduction of ERK/MAPK signaling pathway. Secondly, SHP-2 could promote cell adhesion and cell migration which is of great significance to the combination of seeding cells and scaffolds. SHP-2 can also reduce cell-cell and cell-matrix interactions by reducing the expression of E-cadherin, and can enhance matrix metalloproteinase-1 (MMP-1) and MMP-9 secretion and degradation of extracellular collagen and matrix, providing a favorable condition for cell migration.[44] Moreover, SHP-2 promotes

phosphorylation and focal adhesion kinase (FAK) phosphorylation, thus leading to the reduction of cell adhesion and the increase of cell mobility.[45]

Our research results showed a significant advantage in contrast to the effect of other growth factors in healing calvarial defects in rats. New bone was observed in the left, right, upper, and lower β-TCP boundaries and was almost completely bridged within and across the defects [Fig. 7(A4)]. As a commonly used scaffold in tissue engineering, β-TCP is renowned for its excellent biocompatibility and biodegradability properties. From the stained tissue sections [Fig. 6(A8)], we clearly observed that porosity was less in areas where more bone formed. These findings corresponded well with those of Mastrogiacomo et al.,[46] whereby bone and extracellular matrix formation could facilitate material degradation [Fig. 7(A4) and (A^8)]. Although β-TCP is often criticized for its lack of osteoinductivity and osteogenicity,[47] which restricts its application, this material showed very good osteoinductivity in our histological staining results [Fig. 7(A3,A4,B3,B4)].

Two concerns exist regarding this research. First, SHP-2 plays many different roles in tumor progression, including cell proliferation, DNA damage and replication, apoptosis, invasion and metastasis.[15] We can confirm that there was no evidence of tumor formation observed during experimentation in our study. However, a more in-depth investigation will be carried out in our future research. Second, the specific molecular pathway by which SHP-2 acts requires further investigation. We will also elaborate on this in further studies.

CONCLUSIONS

Our study demonstrates that SHP-2 promoted osteogenic differentiation of BMSCs *in vitro* and that SHP-2 transduced BMSCs combined with β-TCP scaffolds effectively promoted bone regeneration in critical-sized calvarial defects in rats. This study provides evidence for the use of SHP-2 as a potential growth factor for enhanced bone tissue engineering. Further studies will be conducted to evaluate the long-term properties of the bone repair and elucidate more specific molecular mechanisms for the SHP-2 effect on bone.

ACKNOWLEDGMENT

We thank Dr Wang Xiaowen and Qi Zhen for their statistical support. The authors indicate no potential conflicts of interest.

REFERENCES

1. Dailiana ZH, Malizos KN, Varitimidis SE, Urbaniak JR. Donor sites for pedicled skeletal grafts of the hand, wrist, and forearm. Microsurgery 2009;29:408–412.
2. Muramatsu K, Hashimoto T, Tominaga Y, Taguchi T. Vascularized bone graft for oncological reconstruction of the extremities: Review of the biological advantages. Anticancer Res 2014;34: 2701–2707.
3. Cui L, Liu B, Liu G, Zhang W, Cen L, Sun J, Yin S, Liu W, Cao Y. Repair of cranial bone defects with adipose derived stem cells and coral scaffold in a canine model. Biomaterials 2007;28:5477–5486.
4. Ma J, Both SK, Yang F, Cui FZ, Pan J, Meijer GJ, Jansen JA, van den Beucken JJ. Concise review: cell-based strategies in bone tissue engineering and regenerative medicine. Stem Cells Transl Med 2014;3:98–107.
5. Zhao Y-p, Tian Q-y, Frenkel S, Liu C-j. The promotion of bone healing by progranulin, a downstream molecule of BMP-2, through interacting with TNF/TNFR signaling. Biomaterials 2013; 34:6412–6421.
6. Deng Y, Zhou H, Zou D, Xie Q, Bi X, Gu P, Fan X. The role of miR-31-modified adipose tissue-derived stem cells in repairing rat critical-sized calvarial defects. Biomaterials 2013;34:6717–6728.
7. Ben-David D, Srouji S, Shapira-Schweitzer K, Kossover O, Ivanir E, Kuhn G, Muller R, Seliktar D, Livne E. Low dose BMP-2 treatment for bone repair using a PEGylated fibrinogen hydrogel matrix. Biomaterials 2013;34:2902–2910.
8. Qu D, Li J, Li Y, Gao Y, Zuo Y, Hsu Y, Hu J. Angiogenesis and osteogenesis enhanced by bFGF *ex vivo* gene therapy for bone tissue engineering in reconstruction of calvarial defects. J Biomed Mater Res A 2011;96:543–551.
9. Zou D, Zhang Z, He J, Zhu S, Wang S, Zhang W, Zhou J, Xu Y, Huang Y, Wang Y, et al. Repairing critical-sized calvarial defects with BMSCs modified by a constitutively active form of hypoxia-inducible factor-1alpha and a phosphate cement scaffold. Biomaterials 2011;32:9707–9718.
10. Carragee EJ, Hurwitz EL, Weiner BK. A critical review of recombinant human bone morphogenetic protein-2 trials in spinal surgery: emerging safety concerns and lessons learned. Spine J 2011;11:471–491.
11. Tannoury CA, An HS. Complications with the use of bone morphogenetic protein 2 (BMP-2) in spine surgery. Spine J 2014;14: 552−559.
12. Turner N, Grose R. Fibroblast growth factor signalling: From development to cancer. Nat Rev Cancer 2010;10:116−129.
13. Suresh MV, Ramakrishnan SK, Thomas B, Machado-Aranda D, Bi Y, Talarico N, Anderson E, Yatrik SM, Raghavendran K. Activation of hypoxia-inducible factor-1alpha in type 2 alveolar epithelial cell is a major driver of acute inflammation following lung contusion. Crit Care Med 2014;42:e642–e653.
14. Gothard D, Smith EL, Kanczler JM, Rashidi H, Qutachi O, Henstock J, Rotherham M, El Haj A, Shakesheff KM, Oreffo RO. Tissue engineered bone using select growth factors: A comprehensive review of animal studies and clinical translation studies in man. Eur Cell Mater 2014;28:166–207 (discussion 207–208).
15. Zhang J, Zhang F, Niu R. Functions of Shp2 in cancer. J Cell Mol Med 2015;19:2075-2083.
16. Feng GS. Shp2-mediated molecular signaling in control of embryonic stem cell self-renewal and differentiation. Cell Res 2007;17: 37–41.
17. Bauler TJ, Kamiya N, Lapinski PE, Langewisch E, Mishina Y, Wilkinson JE, Feng GS, King PD. Development of severe skeletal defects in induced SHP-2-deficient adult mice: A model of skeletal malformation in humans with SHP-2 mutations. Dis Model Mech 2011;4:228–239.
18. Zambuzzi WF, Milani R, Teti A. Expanding the role of Src and protein-tyrosine phosphatases balance in modulating osteoblast metabolism: Lessons from mice. Biochimie 2010;92:327–332.
19. Tajan M, Batut A, Cadoudal T, Deleruyelle S, Le Gonidec S, Saint Laurent C, Vomscheid M, Wanecq E, Treguer K De Rocca Serra-Nedelec A, et al. LEOPARD syndrome-associated SHP2 mutation confers leanness and protection from diet-induced obesity. Proc Natl Acad Sci USA 2014;111:E4494–E4503.
20. Edwards JJ, Martinelli S, Pannone L, Lo IF, Shi L, Edelmann L, Tartaglia M, Luk HM, Gelb BD. A PTPN11 allele encoding a catalytically impaired SHP2 protein in a patient with a Noonan syndrome phenotype. Am J Med Genet A 2014;164A:2351–2355.
21. Lapinski PE, Meyer MF, Feng GS, Kamiya N, King PD. Deletion of SHP-2 in mesenchymal stem cells causes growth retardation, limb and chest deformity, and calvarial defects in mice. Dis Model Mech 2013;6:1448–1458.
22. Zou GM, Chan RJ, Shelley WC, Yoder MC. Reduction of Shp-2 expression by small interfering RNA reduces murine embryonic stem cell-derived *in vitro* hematopoietic differentiation. Stem Cells 2006;24:587–594.
23. Liu S, Wu J, Liu X, Chen D, Bowlin GL, Cao L, Lu J, Li F, Mo X, Fan C. Osteochondral regeneration using an oriented nanofiber yarn-collagen type I/hyaluronate hybrid/TCP biphasic scaffold. J Biomed Mater Res A 2015;103:581–592.

24. Zhang L, He A, Yin Z, Yu Z, Luo X, Liu W, Zhang W, Cao Y, Liu Y, Zhou G. Regeneration of human-ear-shaped cartilage by co-culturing human microtia chondrocytes with BMSCs. Biomaterials 2014;35:4878–4887.
25. Huang H, Zhang X, Hu X, Shao Z, Zhu J, Dai L, Man Z, Yuan L, Chen H Zhou C, et al. A functional biphasic biomaterial homing mesenchymal stem cells for *in vivo* cartilage regeneration. Biomaterials 2014;35:9608–9619.
26. Liu H, Peng H, Wu Y, Zhang C, Cai Y, Xu G, Li Q, Chen X, Ji J Zhang Y, et al. The promotion of bone regeneration by nanofibrous hydroxyapatite/chitosan scaffolds by effects on integrin-BMP/Smad signaling pathway in BMSCs. Biomaterials 2013;34: 4404–4417.
27. Liu Y, Ming L, Luo H, Liu W, Zhang Y, Liu H, Jin Y. Integration of a calcined bovine bone and BMSC-sheet 3D scaffold and the promotion of bone regeneration in large defects. Biomaterials 2013; 34:9998–10006.
28. Cao L, Liu X, Liu S, Jiang Y, Zhang X, Zhang C, Zeng B. Experimental repair of segmental bone defects in rabbits by angiopoietin-1 gene transfected MSCs seeded on porous beta-TCP scaffolds. J Biomed Mater Res B Appl Biomater 2012;100: 1229–1236.
29. Kasten P, Luginbühl R, van Griensven M, Barkhausen T, Krettek C, Bohner M, Bosch U. Comparison of human bone marrow stromal cells seeded on calcium-deficient hydroxyapatite, β-tricalcium phosphate and demineralized bone matrix. Biomaterials 2003;24: 2593–2603.
30. Tashiro K, Inamura M, Kawabata K, Sakurai F, Yamanishi K, Hayakawa T, Mizuguchi H. Efficient adipocyte and osteoblast differentiation from mouse induced pluripotent stem cells by adenoviral transduction. Stem Cells 2009;27:1802–1811.
31. Ye JH, Xu YJ, Gao J, Yan SG, Zhao J, Tu Q, Zhang J, Duan XJ, Sommer CA Mostoslavsky G., others Critical-size calvarial bone defects healing in a mouse model with silk scaffolds and SATB2-modified iPSCs. Biomaterials 2011;32:5065–5076.
32. Liao YH, Chang YH, Sung LY, Li KC, Yeh CL, Yen TC, Hwang SM, Lin KJ, Hu YC. Osteogenic differentiation of adipose-derived stem cells and calvarial defect repair using baculovirus-mediated co-expression of BMP-2 and miR-148b. Biomaterials 2014;35:4901–4910.
33. Jiang X, Zhao J, Wang S, Sun X, Zhang X, Chen J, Kaplan DL, Zhang Z. Mandibular repair in rats with premineralized silk scaffolds and BMP-2-modified bMSCs. Biomaterials 2009;30:4522–4532.
34. Kamiya N, Kim HK, King PD. Regulation of bone and skeletal development by the SHP-2 protein tyrosine phosphatase. Bone 2014;69:55–60.
35. Urist MR. Bone: Formation by autoinduction. Clin Orthop Relat Res 2002;395:4–10.
36. van den Dolder J, de Ruijter AJ, Spauwen PH, Jansen JA. Observations on the effect of BMP-2 on rat bone marrow cells cultured on titanium substrates of different roughness. Biomaterials 2003; 24:1853−1860.
37. Tazaki J, Murata M, Akazawa T, Yamamoto M, Ito K, Arisue M, Shibata T, Tabata Y. BMP-2 release and dose–response studies in hydroxyapatite and beta-tricalcium phosphate. Biomed Mater Eng 2009;19:141–146.
38. Angle SR, Sena K, Sumner DR, Virkus WW, Virdi AS. Healing of rat femoral segmental defect with bone morphogenetic protein-2: A dose response study. J Musculoskelet Neuronal Interact 2012; 12:28–37.
39. Bodde EW, Boerman OC, Russel FG, Mikos AG, Spauwen PH, Jansen JA. The kinetic and biological activity of different loaded rhBMP-2 calcium phosphate cement implants in rats. J Biomed Mater Res A 2008;87:780−791.
40. Shields LB, Raque GH, Glassman SD, Campbell M, Vitaz T, Harpring J, Shields CB. Adverse effects associated with high-dose recombinant human bone morphogenetic protein-2 use in anterior cervical spine fusion. Spine (Phila Pa 1976) 2006;31:542–547.
41. Jin Y, Zhang W, Liu Y, Zhang M, Xu L, Wu Q, Zhang X, Zhu Z, Huang Q, Jiang X. rhPDGF-BB via ERK pathway osteogenesis and adipogenesis balancing in ADSCs for critical-sized calvarial defect repair. Tissue Eng A 2014;20:3303–3313.
42. Xu D, Xu L, Zhou C, Lee WY, Wu T, Cui L, Li G. Salvianolic acid B promotes osteogenesis of human mesenchymal stem cells through activating ERK signaling pathway. Int J Biochem Cell Biol 2014;51:1–9.
43. Chen Z, Yue SX, Zhou G, Greenfield EM, Murakami S. ERK1 and ERK2 regulate chondrocyte terminal differentiation during endochondral bone formation. J Bone Miner Res 2015;30:765–774.
44. Tang C, Luo D, Yang H, Wang Q, Zhang R, Liu G, Zhou X. Expression of SHP2 and related markers in non-small cell lung cancer: A tissue microarray study of 80 cases. Appl Immunohistochem Mol Morphol 2013;21:386−394.
45. Hartman ZR, Schaller MD, Agazie YM. The tyrosine phosphatase SHP2 regulates focal adhesion kinase to promote EGF-induced lamellipodia persistence and cell migration. Mol Cancer Res 2013; 11:651–664.
46. Mastrogiacomo M, Papadimitropoulos A, Cedola A, Peyrin F, Giannoni P, Pearce SG, Alini M, Giannini C, Guagliardi A, Cancedda R. Engineering of bone using bone marrow stromal cells and a silicon-stabilized tricalcium phosphate bioceramic: Evidence for a coupling between bone formation and scaffold resorption. Biomaterials 2007;28:1376–1384.
47. Liu B, Lun DX. Current application of beta-tricalcium phosphate composites in orthopaedics. Orthop Surg 2012;4:139–144.